

Are your **MRI contrast agents** cost-effective?

Learn more about generic **Gadolinium-Based Contrast Agents**.



FRESENIUS
KABI

caring for life

AJNR

MR of visual pathways in patients with neurofibromatosis.

S J Pomeranz, J J Shelton, J Tobias, K Soila, D Altman and M Viamonte

AJNR Am J Neuroradiol 1987, 8 (5) 831-836

<http://www.ajnr.org/content/8/5/831>

This information is current as of April 30, 2024.

MR of Visual Pathways in Patients with Neurofibromatosis

Stephen J. Pomeranz^{1,2}
 Jerome J. Shelton
 Jeffrey Tobias
 Kalevi Soila
 Donald Altman
 Manuel Viamonte

MR was performed on six patients clinically diagnosed as having neurofibromatosis. Owing to its multiplanar capability, MR greatly helped determine the extent of visual pathway disease. We attempted to find specific optimal pulse sequences for evaluating the prechiasmatic, chiasmatic, and retrochiasmatic visual system at 0.35 T. Using spin-echo techniques, we evaluated a T1-weighted sequence (TR 300 msec/TE 35 msec), an intermediate T2-weighted sequence (TR 1500 msec/TE 35 msec), and a T2-weighted sequence (TR 1500 msec/TR 70 msec).

We found that the orbital and intracranial optic nerves were most accurately and easily seen with the T1-weighted sequence axially and coronally; the chiasm was best seen with the intermediate T2-weighted coronal sequence; and the retrochiasmatic visual pathway was optimally evaluated with T2-weighted spin-echo technique.

Neurofibromatosis (von Recklinghausen's disease) is a familial condition transmitted as an autosomal dominant and resulting from dysplasia of mesoderm and neuroectoderm. Approximately 50% of the cases arise as spontaneous mutation. The estimated frequency is one in 3,000 births [1].

CNS neoplasms associated with neurofibromatosis include optic nerve glioma, trigeminal nerve neuroma, acoustic nerve neuroma, meningioma, astrocytoma, ependymoma, hamartoma, and glioblastoma [2]. Among patients with neurofibromatosis, 16% have an optic nerve glioma and 30–37% with chiasmatic or optic nerve gliomas exhibit other manifestations of von Recklinghausen's disease [3, 4]. Only 25% of all cases of optic gliomas present after age 10, and 25% of all patients manifest a more extensive disease involving not only the optic nerve but also the optic chiasm, optic tract, lateral geniculate nucleus, and optic radiation [5]. We performed MR imaging on six patients clinically diagnosed as having neurofibromatosis. These patients presented with precocious puberty and/or visual field deficits. The ability of MR to detect disease in the orbital and intracranial optic nerves, chiasm, hypothalamic, and retrochiasmatic visual pathway was compared with CT. Spin-echo technique using T1-weighted (TR 300 msec/TE 35 msec), intermediate T2-weighted (TR 1500 msec/TE 35 msec), and T2-weighted (TR 1500 msec/TE 70 msec) sequences was tested in each of the anatomic sites in multiple projections using a 0.35 T system.

Subjects and Methods

We performed over 1,000 MR examinations in 1984. Six patients ranging in age from 5 to 12 years and clinically diagnosed as having neurofibromatosis underwent MR of the brain. Among these, three were thought to have possible precocious puberty secondary to hypothalamic disease and three were being examined for optic chiasm or tract abnormalities (Figs. 1, 2, 3) suspected on CT. One of the six patients was also being evaluated for a long-standing right hemiparesis incurred at age 2 as a result of cerebral vascular occlusion in the left middle cerebral artery distribution (Fig. 4). Although none of the patients had pathologic confirmation of their intracranial abnormalities, all had known neurofibromatosis with clinical and radi-

Received January 30, 1985; accepted after revision April 27, 1987.

¹ All authors: Department of Radiology, Mount Sinai Medical Center, 4300 Alton Rd., Miami Beach, FL 33140.

² Present address: Department of Radiology, The Christ Hospital, 2139 Auburn Ave., Cincinnati, OH 45219. Address reprint requests to S. J. Pomeranz.

AJNR 8:831–836, September/October 1987
 0195–6108/87/0805–0831

© American Society of Neuroradiology



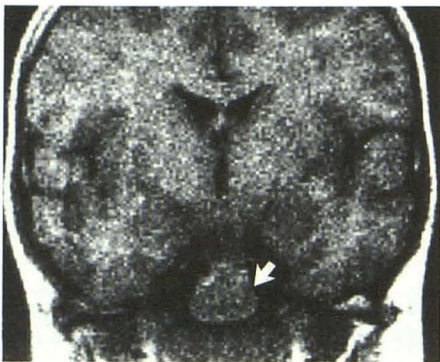
A

Fig. 1.—9-year-old boy with a poorly defined visual deficit.
 A, Axial noncontrast CT shows a suprasellar mass of slightly increased attenuation when compared with normal brain parenchyma (*arrow*).

B, Coronal T1-weighted MR (TE 35 msec/TR 300 msec) through sella and suprasellar region. Mass (*arrow*) involves both sellar and suprasellar regions.

C, Sagittal intermediate T2-weighted MR (TE 35 msec/TR 1500 msec) most clearly demonstrates sellar extent (*large arrow*), anterior hypothalamic extension (*small arrow*), and involvement of mamillary body region (*arrowhead*).

D, Sagittal T2-weighted MR (TE 70 msec/TR 1500 msec) provides little tissue contrast between CSF, brain, and optic chiasm glioma (*arrows*).



B



C



D

ographic findings characteristic of optic system disease. The MR system used in these studies was a superconducting magnet operating at 0.35 T (Siemens, West Germany) using a two-dimensional Fourier transform technique of reconstruction.

Patients were asked to close their eyes during image acquisition. Sagittal, axial, and coronal images were obtained with both 5-mm and 10-mm section thicknesses. Spin-echo (SE) techniques with T1-weighted (TR 300 msec/TE 35 msec), intermediate T2-weighted (TR 1500 msec/TE 35 msec), and T2-weighted (TR 1500 msec/TE 70 msec) images were tested in optic nerves, chiasm, and retrochiasm regions. Data acquisition times varied with the pulse sequence, matrix size, and number of averages per sequence, ranging from 3.5 to 12.7 min.

One patient had cerebral angiography, and all patients had cranial CT with and without IV contrast. MR and CT were compared anatomically on a section-by-section basis.

Results

Sagittal scout sections were obtained using a T1-weighted spin-echo image (TR 300 msec/TE 35 msec) with two averages. This not only allowed "tailoring" of the remainder of the examination, but also provided T1 information about the optic tract, sellar region, and hypothalamus in the sagittal plane.

Maximal visualization of the optic nerves was provided by 5-mm coronal T1-weighted (TR 300 msec/TE 35 msec) images (Fig. 2D) with four averages (6.9 min). The contrast accentuation provided by the short T1 of periorbital fat allowed visualization of the optic nerves, which have a moderate T1 compared with fat [6]. Selection of 5-mm sections and a TR of 300 msec allowed good spatial resolution, short imaging times, and acceptable signal/noise characteristics. Chiasmatic and optic tract disease (Figs. 1–3) was best defined with the intermediate T2 (TR 1500 msec/TE 35 msec) 5-mm coronal images with two excitations (12.7 min). Using this pulsing sequence, CSF remained of low signal intensity and contrasted the bright signal of optic chiasm and tract glioma at 0.35 T. Excellent signal/noise characteristics allowed thin-section (5-mm) imaging and good spatial resolution. Since contour abnormalities are as important as contrast abnormalities in chiasmatic evaluation at 0.35 T, this is an important point.

Prechiasmatic and chiasmatic optic gliomas exhibited virtual isointensity as compared with normal brain using T1-weighted sequences and minimal to moderate increased signal relative to brain using T2-weighted spin-echo sequences. Spin-echo images at TR 1500 msec/TE 70 msec optimized

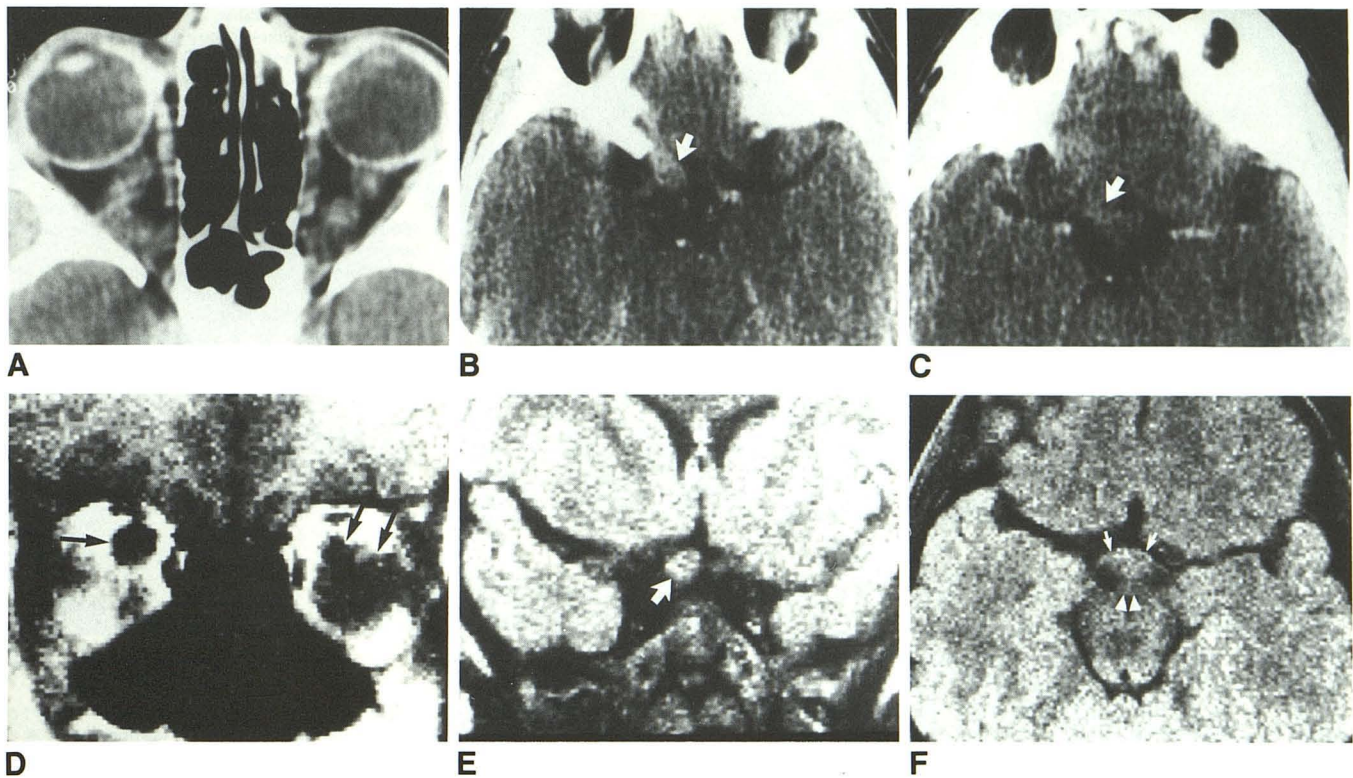


Fig. 2.—10-year-old boy with complex visual field deficits and a questionable history of precocious puberty.

A, Axial noncontrast CT shows bilateral optic nerve enlargement and lobulation.

B, Axial contrast-enhanced CT at suprasellar level. Intracanalicular optic nerve glioma extends toward region of right side of optic chiasm (arrow).

C, Axial contrast-enhanced CT shows a chiasmatic suprasellar mass (arrow) whose exact borders cannot be distinguished.

D, Coronal T1-weighted MR (TE 35 msec/TR 300 msec). Pronounced bilateral optic nerve enlargement (arrows) is highly contrasted with bright signal of surrounding periorbital fat.

E, Coronal intermediate T2-weighted MR (TE 35 msec/TR 1500 msec) shows enlargement of right portion of optic chiasm (arrow). On this sequence, abnormality is highly contrasted with surrounding CSF and bone.

F, Axial intermediate T2-weighted MR (TE 35 msec/TR 1500 msec) shows chiasmatic glioma (arrows) anterior to mammillary bodies (arrowheads). Chiasmatic borders are well outlined.

tissue contrast between abnormalities in the optic radiation of thalamus and surrounding brain (Fig. 3D). At the field strength of our system, the crossover point at which chiasm and brain became isointense with CSF approached TR 1500 msec/TE 70 msec. Therefore, spin-echo images provided little or no tissue contrast between CSF and optic chiasm glioma at this particular sequence (Fig. 1D).

Three patients were evaluated for possible precocious puberty; MR delineated normal anatomy in the chiasmatic, hypothalamic, and mammillary body regions in one patient and detected abnormalities that went unrecognized by CT in the remaining two patients. Central endocrine abnormalities were subsequently confirmed by laboratory parameters in the latter two patients. One of these two exhibited a focus of increased signal on T2-weighted images in the region of the basal ganglia and subthalamus, which had been inadequately visualized on CT (Fig. 4). This corresponded to a site of previous cerebral infarction and current neurologic deficit. Also, a chiasmatic mass was suspected by CT; however, MR clearly demonstrated normal optic nerves, chiasm, and tract. The third patient had a normal subthalamus and hypothalamus

but bilateral optic nerve gliomas and a large chiasmatic mass were demonstrated on both CT and MR (Fig. 2).

A patient with visual field deficits was found to have a chiasmatic mass on CT. Clinical findings suggested more extensive retrochiasmatic disease. A chiasmatic mass extending into the left optic tract, left lateral geniculate body, and left optic radiation was evident on T2-weighted spin-echo images, but only a calcified left-sided thalamic mass was imaged on CT (Fig. 3).

Discussion

Reports of MR in patients with neurofibromatosis or with visual pathway gliomas are scant [7, 8]. Some authors consider optic pathway glioma and neurofibromatosis to be a congenital nonneoplastic hamartoma. The occurrence has been slightly more frequent in females than males, and chiasmatic disease appears to be more common than optic nerve pathology [8–10]. It has been suggested that retrochiasmatic gliomas exhibit more aggressive behavior than prechiasmatic

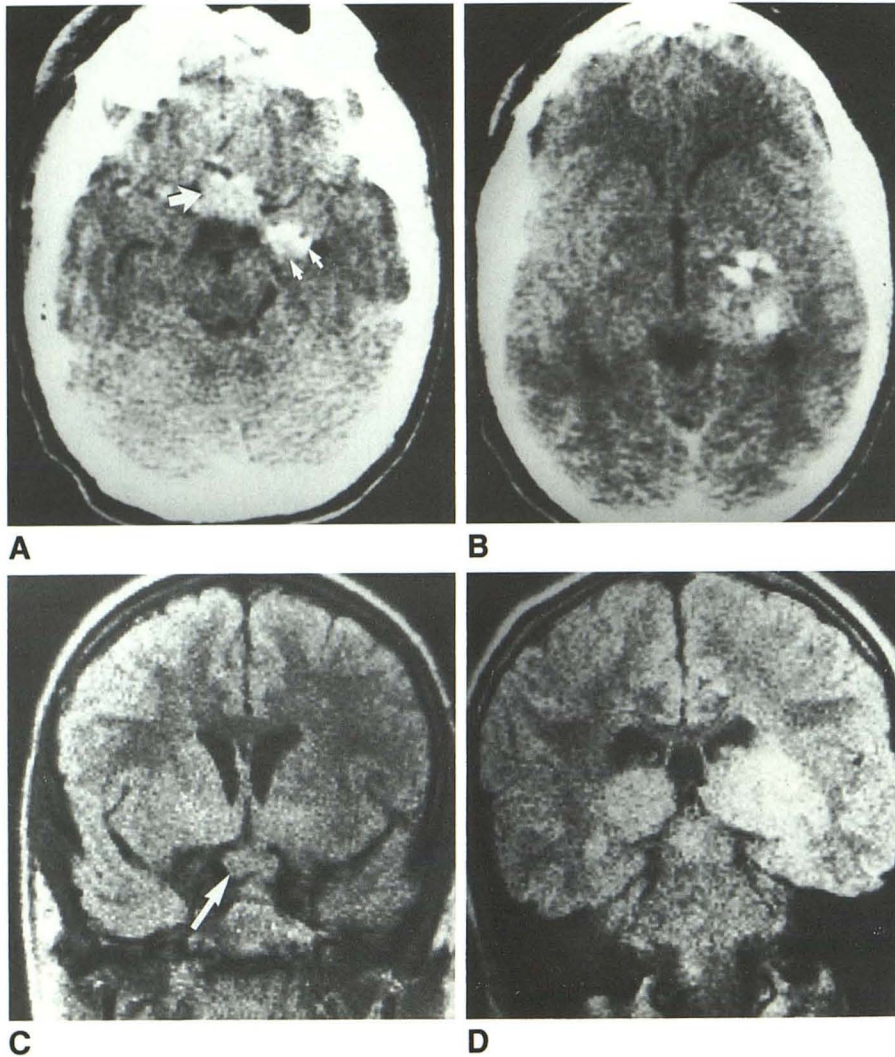


Fig. 3.—Progressive, complex visual disturbance in this 5-year-old boy was noted.

A, Noncontrast axial CT shows calcified suprasellar mass (*large arrow*) with extension toward left optic radiation and lateral geniculate body region (*small arrows*).

B, Axial noncontrast CT shows area of increased attenuation and calcification in left thalamic and lenticular nucleus regions.

C, Coronal T2-weighted MR (TE 35 msec/TE 1500 msec) shows bilateral chiasmatic glioma (*arrow*).

D, Coronal intermediate T2-weighted MR (TE 35 msec/TR 1500 msec) shows retrochiasmatic extension of gliomatous process into and beyond geniculate body, involving left optic radiation.

gliomas, and often extend into the region of the hypothalamus and third ventricle.

Gliomas of the optic nerve manifest themselves clinically by early axial, nonpulsatile proptosis; increased resistance to orbital retropulsion; and severe visual loss at the time of diagnosis [11]. Optic nerve atrophy is more common than papilledema; visual field deficits are of the central scotoma type with increasing hypermetropia, and they result from pressure of the tumor on the globe's posterior surface. Orbital meningiomas occurring in neurofibromatosis exhibit proptosis, but less frequent increased resistance to retropulsion of the globe and visual field deficits occur later.

Visual loss begins earlier in patients with chiasmatic disease than in those with intraorbital glioma. Signs and symptoms of increased intracranial pressure, hypopituitarism, obesity, dwarfism, diabetes insipidus, and precocious puberty may occur with invasion of the third ventricle and hypothalamus [9].

In our patients being evaluated for precocious puberty, MR clearly demonstrated whether gliomatous invasion of the hy-

pothalamus and surrounding structures was present. CT was suboptimal in depicting the anatomy of this region. MR differentiated the normal and abnormal chiasm more distinctly than CT. Moreover, MR depicted a normal chiasm in a patient who by CT was thought to have a possible chiasmatic tumor. MR also demonstrated an old, left middle cerebral infarction not previously recognized. MR outlined the extent of retrochiasmatic disease in the optic tracts, lateral geniculate nucleus, and optic radiation, whereas CT did not clearly visualize these features. Optimal imaging pulse sequences using spin-echo at lower field strengths are still being determined. Optic nerve pathology was best seen with T1-weighted spin-echo images (TR 300 msec/TE 35 msec). The short T1 relaxation times of retroorbital fat provided excellent contrast surrounding the moderately long T1 relaxation times (approximately equal to brain tissue) and T2 relaxation times (minimally prolonged as compared with brain) of optic nerve pathology. Sections that were 5 mm thick, that possessed a TR of 300 msec, and had four excitations provided the optimal compromise between spatial and contrast resolution, imaging time, and signal/noise

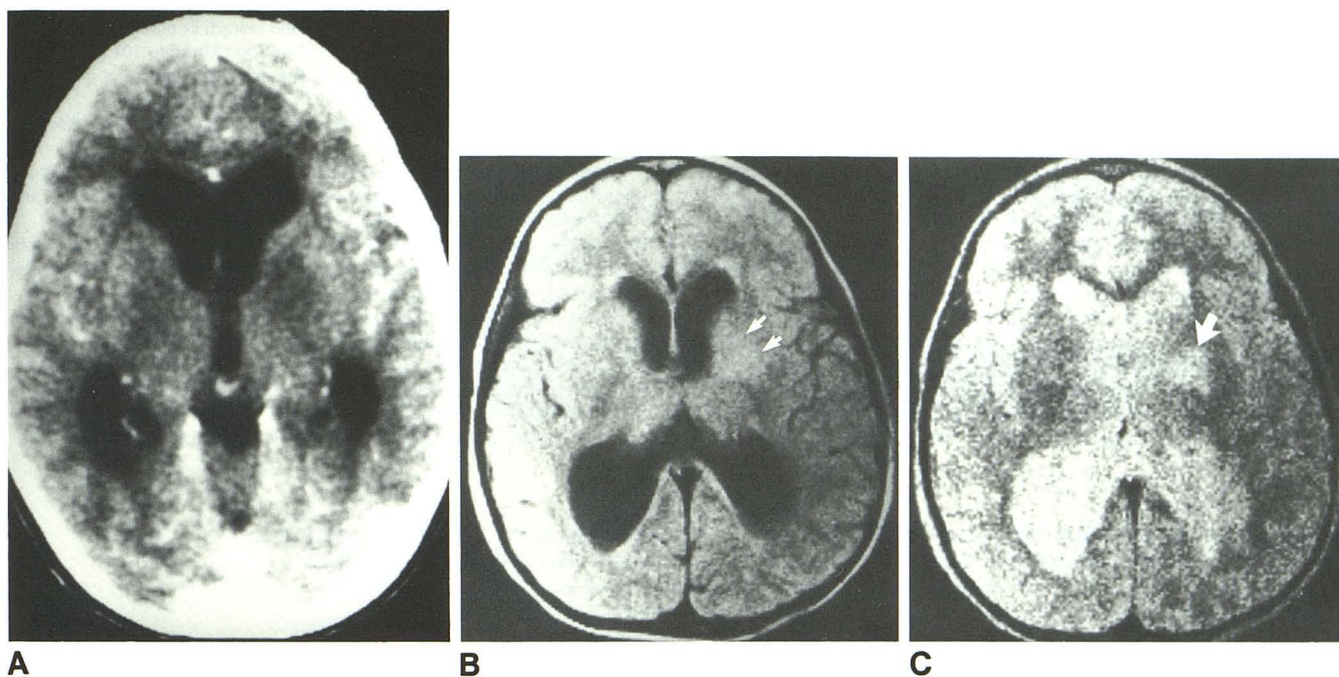


Fig. 4.—6-year-old girl with seizures since age 2.
A, Axial contrast CT shows moderate ventricular dilatation only.
B, Axial intermediate T2-weighted MR (TE 35 msec/TR 1500 msec) shows a focus of increased signal in left lenticular nucleus region (arrows).
C, Axial T2-weighted MR (TE 70 msec/TR 1500 msec) better demonstrates left lenticular nucleus abnormality (arrow) that proved to be an old, left middle cerebral artery infarction.

ratio. Daniels et al. [6] recommended coronal partial saturation recovery (SR) sequences for imaging the optic nerves and chiasm; however, their results were obtained using 0.5, 1.0, and 1.5 T units. MR imaging sequence selection in suprasellar and chiasmatic regions may differ at higher field strengths since the crossover point differs from that obtained at 0.35 T [6, 12].

At the field strength used, the intermediate T2-weighted spin-echo sequence (TR 1500 msec/TE 35 msec) gave the optimal chiasmatic/CSF contrast. Since the crossover point on our unit approaches TR 1500 msec/TE 70 msec, this sequence provided no chiasmatic/CSF tissue contrast. The intermediate T2-weighted image, using an echo time of 35 msec, provided excellent signal-to-noise ratio, contrast, and spatial resolution. Retrochiasmatic disease in the lateral geniculate nucleus and optic radiation was best seen on T2-weighted spin-echo images (TR 1500 msec/TE 70 msec). This provided the greatest glioma/normal brain contrast of the sequences examined at 0.35 T.

There are some specific advantages to the use of MR besides its ability to determine the extent of hypothalamic and retrochiasmatic invasion in patients with related symptoms. The following factors should be taken into consideration: (1) the examination delivers no ionizing radiation or IV contrast; (2) bone and nonferromagnetic metallic implants such as gold and dental amalgam, often a problem in direct coronal CT of the sellar region, produce no artifacts [13]; (3)

MR allows direct coronal and sagittal imaging, and in many instances yields better spatial orientation of intracranial pathology. MR's sensitivity in depicting intracranial pathology may be greater than that of CT [7, 14–16].

In summary, optimal pulsing sequences at 0.35 T when imaging the visual pathways included T1-weighted (TR 300 msec/TE 35 msec) axial and coronal 5-mm sections of the optic nerves, intermediate T2-weighted (TR 1500 msec/TE 35 msec) coronal 5-mm sections of the chiasm, and T2-weighted (TR 1500 msec/TE 70 msec) axial and coronal images in the retrochiasmatic region. We acknowledge the fact that thinner sections using higher field strengths will likely allow greater spatial resolution with little decrease in signal/noise ratio. Also, we are aware that the crossover point between CSF and brain will differ with stronger magnets, thus altering optimal sequences for chiasmatic imaging.

Specific anatomic delineation of optic glioma is important in confirming unexplained endocrine and visual deficits. Chiasmatic and retrochiasmatic disease portends more aggressive disease and thus a poorer prognosis [2, 4, 5, 9]. An accurate, specific diagnosis by MR assists in medical management and psychological counseling.

ACKNOWLEDGMENTS

We are indebted to Joseph Weinstein and Sheila Caplin for technical assistance and preparation of this manuscript.

REFERENCES

1. Crowe FW, Schull WJ, Neel JV. *A clinical, pathological and genetic study of multiple neurofibromatosis*. Springfield, IL: Thomas, **1948**
2. Kallate EC, Franken EA, Smith JA. The radiographic spectrum in neurofibromatosis. *Semin Roentgenol* **1976**;11:17-33
3. Marshall D. Glioma of the optic nerve, manifestation of Von Recklinghausen's disease. *Am J Ophthalmol* **1954**;37:15
4. Lloyd LA. Gliomas of the optic nerve and chiasm in childhood. *Trans Am Ophthalmol Soc* **1973**;71:488
5. Zimmerman RA, Bilaniuk LT. The orbit. In: Lee SH, Raho KJVG, eds. *Cranial computed tomography*. New York: McGraw Hill, **1983**:95
6. Daniels DL, Herfkins R, Gager WE, et al. Magnetic resonance imaging of the optic nerves and chiasm. *Radiology* **1983**;152:79-83
7. Brant-Zawadzki M, Norman D, Newton TH, et al. Magnetic resonance of the brain: the optimal screening technique. *Radiology* **1984**;152:71-77
8. Horvath K, Fink I, Patronas NJ, Bader J. MR characterization of neurofibromas and neurofibrosarcoma. *Radiology* **1984**;153 (P):307
9. Lloyd LA. Gliomas of the optic nerve and chiasm in childhood. In: Smith JL, ed. *Neuroophthalmology update*. New York: Masson, **1977**: 185-198
10. Miller NR, Iliff WJ, Green WR. Evaluation and management of gliomas of the anterior visual pathway. *Brain* **1974**;97:943
11. Walsh FB, Hoyt WF. *Clinical Neuro-ophthalmology*. Baltimore: Williams & Wilkins, **1969**:2076
12. Modic MT, Weinstein MA, Pavlicek W, Boumpfrey F, Starnes D, Duchesneau PM. Magnetic resonance imaging at the cervical spine: technical and clinical observations. *AJR* **1983**;141:1129-1136; *AJNR* **1984**;5:15-22
13. New PJ, Rosen BR, Brady TJ, et al. Potential hazards and artifacts ferromagnetic and nonferromagnetic surgical and dental materials and devices in nuclear magnetic resonance. *Radiology* **1983**;147:139-148
14. Han JJ, Bonstelle CT, Kaufman B, et al. Magnetic resonance imaging in the evaluation of the brain stem. *Radiology* **1984**;150:705-712
15. Lee BP, Kneeland JP, Deck MDF, Cahill PT. Posterior fossa lesions: magnetic resonance imaging. *Radiology* **1984**;153:137-143
16. Pomeranz SJ, Soila K, Tobias J, Sheldon JJ, Ros P, Viamonte M. Sensitivity of MRI in metastatic neoplasia. *Mag Res Imag* **1985**;3:291-293